JMEPEG (2015) 24:3798–3807
DOI: 10.1007/s11665-015-1707-7

1059-9495/$19.00

Development of High Performance Magnesium Matrix Nanocomposites Using Nano-SiC Particulates as Reinforcement

M.J. Shen, W.F. Ying, X.J. Wang, M.F. Zhang, and K. Wu

(Submitted June 28, 2015; in revised form August 6, 2015; published online September 9, 2015)

In the present study, magnesium-based composites with three different volume percentages of nano-sized SiC particulates (SiCp) reinforcement were fabricated using a simple and inexpensive technique followed by hot extrusion. Microstructural characterization of the materials revealed uniform distribution of nano-size SiCp and obvious grain refinement. The tensile test result indicates a remarkable improvement on the strength for the as-extruded SiCp/AZ31B nanocomposite, while the elongation to fracture was decreased by comparing with the AZ31B alloy. Although, compared with the as-extruded AZ31B alloy, the ductility of the SiCp-reinforced AZ31B nanocomposite is decreased, but the ductility of the present SiCp-reinforced AZ31B nanocomposite is far higher than that of the conventional micron or submicron SiCp-reinforced magnesium matrix composites. It is concluded that, compared with the larger sized (micron or submicron) particles, the addition of nano SiCp in the AZ31B alloy resulted in the best combination of the strength and ductility. An attempt is made in the present study to correlate the effect of presence of nano-SiCp as reinforcement and its increasing amount with the microstructural and mechanical properties of magnesium.

Keywords magnesium matrix nanocomposite, mechanical properties, microstructure

1. Introduction

In order to improve the mechanical properties of the magnesium, the substantial efforts have been carried out to develop the magnesium matrix composites due to their higher specific strength and stiffness, higher wear resistance, and creep resistance as well as the improved high temperature properties. Among different reinforcement reinforced magnesium matrix composites, the reinforcements with low cost and practicability are usually silicon carbide and alumina particles (Ref 1, 2). Compared with the unreinforced magnesium alloy, the conventional micron particles-reinforced magnesium matrix composites normally possess much higher tensile strength and elastic modulus, but their defects are also remarkable. Generally, the tensile strength of the micron particle-reinforced magnesium matrix composite is increased only when the content of micron particle is high, i.e., the reinforcing efficiency of the micron particle-reinforced magnesium matrix composite is low. At the same time, the ductility of the micron particle-reinforced magnesium matrix composite is also disappointingly deteriorated. Wang et al.'s study (Ref 3) on the tensile behavior of the magnesium alloy (AZ91D) reinforced with micron SiCp indicates that the 350R12 extruded composite provided the 252 MPa yield strength and the 335 MPa ultimate tensile strength, while the elongation was decreased to 3% (elongation of extruded AZ91D alloy: ~18%). Nie et al. (Ref 4) used the multidirectional forging method to prepare the bulk fine grain structural micron SiCp (10 vol.%)/AZ91 magnesium matrix composite with relatively high strength, but the elongation of composite was decreased to 1.4%. These main drawbacks limit the micron particles-reinforced magnesium matrix composites to be widely applied and developed. At present, the expected properties can be obtained by using the various particulates including the nano-sized particles. Many literatures indicate that the nano particle-reinforced magnesium matrix composites have triggered great research interests because of the potential development and the advantages of the novel composites with unique mechanical and physical properties (Ref 5, 6). Hassan et al. (Ref 7) used the innovative disintegrated melt deposition technique and the blend-press-sinter powder metallurgy technique to obtain the nanocomposites with 0.2 and 0.7 vol.% of 29-nm Y_2O_3 particulates, and then the cast billets were hot extruded. In their works, the extruded 0.7 vol.%-Y_2O_3/Mg matrix composite provided the 312 MPa yield strength (σ_{YS}) and the 318 MPa ultimate tensile strength (σ_{UTS}), while the elongation to fracture was increased to 6.9% (micron SiCp/Mg matrix composites: $<4\%$). Gupta et al.'s (Ref 8) study illustrated that, compared to the AZ91 magnesium alloy reinforced with much higher content of micron sized SiCp, the 0.2% yield strength, ultimate tensile strength, and ductility of the magnesium matrix nanocomposites containing 1.11 vol.% of alumina particle were remain higher. And the 1.11 vol.%-Al_2O_3/Mg matrix composite provided the 194 MPa yield strength (σ_{YS}), 250 MPa ultimate tensile strength (σ_{UTS})

M.J. Shen, College of Engineering, Shenyang Agricultural University, Shenyang 110866, People's Republic of China; **W.F. Ying**, College of Chemical Engineering and Materials Science, Eastern Liaoning University, Dandong 118003, People's Republic of China; **X.J. Wang** and **K. Wu**, School of Materials Science and Engineering, Harbin Institute of Technology, Harbin 150001, People's Republic of China; and **M.F. Zhang,** Liaoning Provincial Gem Quality Supervision and Inspection Center, Shenyang 110000, People's Republic of China. Contact e-mails: smjiekaka@163.com and yingweifengneu@163.com.

and 6.8% elongation to fracture. Nie et al. (Ref 9) fabricated nano-SiCp/AZ91D composites by stir casting method, and it was found that the tensile properties of the AZ91D magnesium alloy increased with the increase of smaller sized nano SiCp content. However, when the nano SiCp (~60 nm) content exceeded 1 vol.%, the agglomeration regions appeared in the composites, and the tensile properties were obviously decreased. Obviously, the mechanical properties of the composites tend to be improved with increasing volume fraction and decreasing particle size. However, the result of literature search indicates that it is extremely challenging for the cheapest and the simplest technique to manufacture nano particle-reinforced magnesium matrix composites, especially the nano SiC particle with high volume content are uniformly dispersed in the magnesium melts. Moreover, so far very limited attempts are carried out to increase the strength and ductility of magnesium simultaneously by introducing high volume content of nano SiCp.

Accordingly, the primary aim of the present study is to synthesize different content nano-SiCp-reinforced magnesium matrix composites by using the semisolid stirring assisted ultrasonic vibration technique. The microstructures and the mechanical properties of the nanocomposites before and after hot extrusion have been evaluated and characterized. The particular emphasis is placed to study the effect of presence of nano-sized SiCp and its increasing amount on the microstructure and the mechanical response of the AZ31B magnesium alloy.

2. Materials and Methods

Industrial AZ31B magnesium alloy (supplied by Northeast Light Alloy Company Limited, China) with a nominal composition of Mg-2.8Al-0.8Zn-0.3Mn (wt.%) was used as the matrix. The nano SiC particulate (supplied by Nano Energy Technology Company Limited, China) with the average size of 60 nm was used as the reinforcement. The nano SiCp-reinforced AZ31B magnesium matrix composites (SiCp/AZ31B nanocomposites) containing three volume fractions (1, 2, 3 vol.%) were fabricated by semisolid stirring assisted ultrasonic vibration. The details of the fabrication process were given in our previous work (Ref 10). After homogenized at 400 °C for 12 h, the all billets were extruded at 350 °C with the extrusion ratio of 12:1. In order to identify the effect of nano SiCp on the microstructure and the mechanical properties of composites, the monolithic AZ31B alloy was also prepared by the same fabrication method. The microstructure and the mechanical properties of the AZ31B alloy before and after hot extrusion were given in our previous works (Ref 10, 11).

The optical microscopy (OM) (P-3, Olympus, Japan), scanning electron microscopy (SEM) (Quanta 200FEG, FEI Co.Ltd., USA), and transmission electron microscopy (TEM) (HR-TEM, Tecnai G^2 F30, USA) were applied to study the microstructure of matrix and the distribution of nano SiCp before and after hot deformation. Microstructural features of the SiCp/AZ31B nanocomposite were identified using energy dispersive spectrophotometric (EDS) analysis. The specimens for the microstructure analysis were sectioned parallel to the extrusion direction (ED) and prepared by the conventional mechanical grinding, polishing and etched in the acetic picral [2 ml acetic acid + 2 g picric acid + 20 ml ethanol (95%)]. The average grain size of each sample was obtained by using the mean linear intercept method. The linear intercept length of at least 2500 matrix grains in the SiCp/AZ31B nanocomposite was determined by using the Image-Pro Plus (IPP) software. The specimens for TEM tests were made into a foil of 50 μm thickness by grinding-polishing and followed ion beam thinned. The tensile tests were carried out by using an Instron-5569 universal testing machine at a constant crosshead speed of 0.5 mm/min. Each material for repeat tensile tests was cut into three samples with the standard dog-bone shape parallel to the extrusion direction. The dimensions of the tensile specimens were given in the previous work (Ref 11).

3. Results and Discussion

3.1 Microstructures of As-Cast SiCp/AZ31B Nanocomposites

Figure 1 illustrates the SEM micrographs of the as-cast SiCp/AZ31B nanocomposites. It can be observed from the low magnification in Fig. 1 that the distribution of nano SiCp is typical necklace particle distribution. It can be attributed to the "push" effect of the liquid-solid interface during the solidification (Ref 12). This is very normal for the metal matrix composites fabricated by melt stirring technology. It also can be seen from Fig. 1 that the amount of nano SiCp was increased with increasing the volume fraction of nano SiCp. For the 3 vol.%-SiCp/AZ31B nanocomposite. Moreover, a small number of bright white phases were observed, which was correspond to the second phase ($Mg_{17}Al_{12}$) in the present SiCp/AZ31B nanocomposites (as indicated by arrows in Fig. 1a). Figure 1(d) is the magnified SEM image of the 3 vol.%-SiCp/AZ31B nanocomposite. The particle-rich regions correspond to the intergranular regions and most of the SiCp exhibited the typical "island" distribution within the intergranular regions. It should be noted that the "island" distribution causes serious stress concentrations under external load, and then usually impairs the mechanical properties of composite (Ref 2, 5). Therefore, it is necessary to eliminate the casting defects and redistribute the particles by applying hot deformation. In addition, the n-SiCp cannot be clearly found because of the smaller particle size (~60 nm). Therefore, the further magnified TEM images analysis is required in present work, as shown in Fig. 2.

Figure 2 shows the TEM graphs of the 3 vol.%-SiCp/AZ31B nanocomposite. There are two kinds of zones in the as-cast SiCp/AZ31B nanocomposite: SiCp-rich zone and SiCp-poor zone. The amount of nano SiCp in the SiCp-rich zone is more than that in the SiCp poor zone, while the macroscopic clusters of SiCp within the nano SiCp rich zone were not observed. Moreover, Fig. 2(a) illustrates that most of nano SiCp within the nano SiCp rich zone were still segregated by matrix. It means that nano SiCp can be further uniformly dispersed by hot extrusion. The study electron diffraction in Fig. 2(b) illustrates that the composition of the particles is nano SiCp, and nano SiCp is β-SiCp of face-centered cubic structure.

Figure 3 illustrates the OM micrographs of the as-cast SiCp/AZ31B nanocomposites. Figure 4 shows the average grain size of the as-cast SiCp/AZ31B nanocomposites with different volume fractions of nano SiCp. Compared with the as-cast AZ31B alloy (Ref 10), the grains in all the SiCp/AZ31B

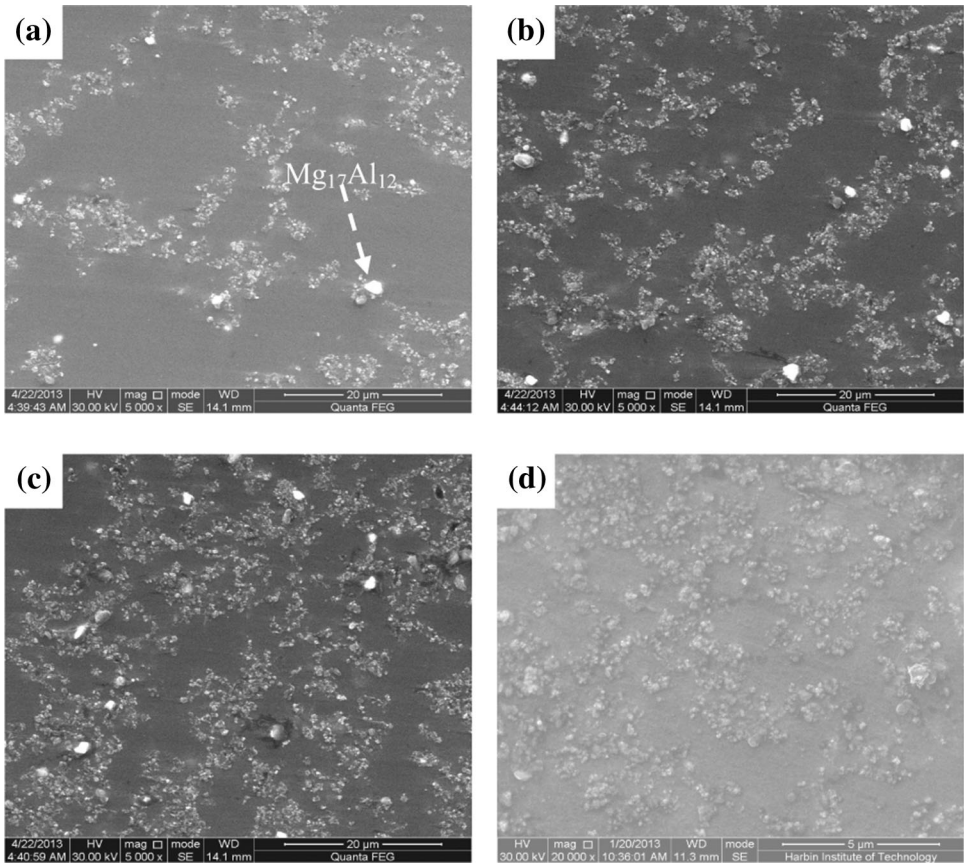

Fig. 1 SEM micrographs of as-cast SiCp/AZ31B nanocomposites: (a) 1 vol.% SiCp/AZ31B nanocomposite, (b) 2 vol.% SiCp/AZ31B nanocomposite, (c) 3 vol.% SiCp/AZ31B nanocomposite, (d) high magnification of (c)

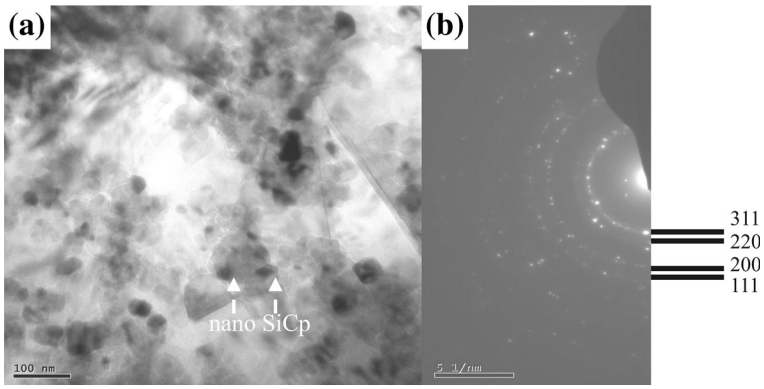

Fig. 2 TEM micrographs of the as-cast 3 vol.%-SiCp/AZ31B nanocomposite: (a) distribution of nano SiCp, (b) electron diffraction of nano SiCp

nanocomposites were refined. This illustrates that the addition of nano SiCp has a significant effect on refining grain. With increasing the volume fraction of nano SiCp, the grains in the SiCp/AZ31B nanocomposites were gradually refined. In addition, by combining Fig. 1 and 3, it can be found that most of the nano SiCp were segregated within the intergranular regions in the as-cast SiCp/AZ31B nanocomposites. It can be explained that most of nano SiCp were pushed ahead by liquid-solid interface during the growth of primary magnesium grains, which result from the fabricating method. When impinged with other growing grains, these particles were segregated in the intergranular regions (Ref 13). Moreover, it can be seen from the high and low magnified OM graphs in Fig. 3 that the particle macro-clusters were not observed, which is consistent with the observation of SEM micrographs in the as-cast SiCp/AZ31B nanocomposites in Fig. 1.

3.2 Microstructures of As-Extruded SiCp/AZ31B Nanocomposites

The optical micrographs of the SiCp/AZ31B nanocomposites after hot extrusion are shown in Fig. 5. Figure 6 shows the

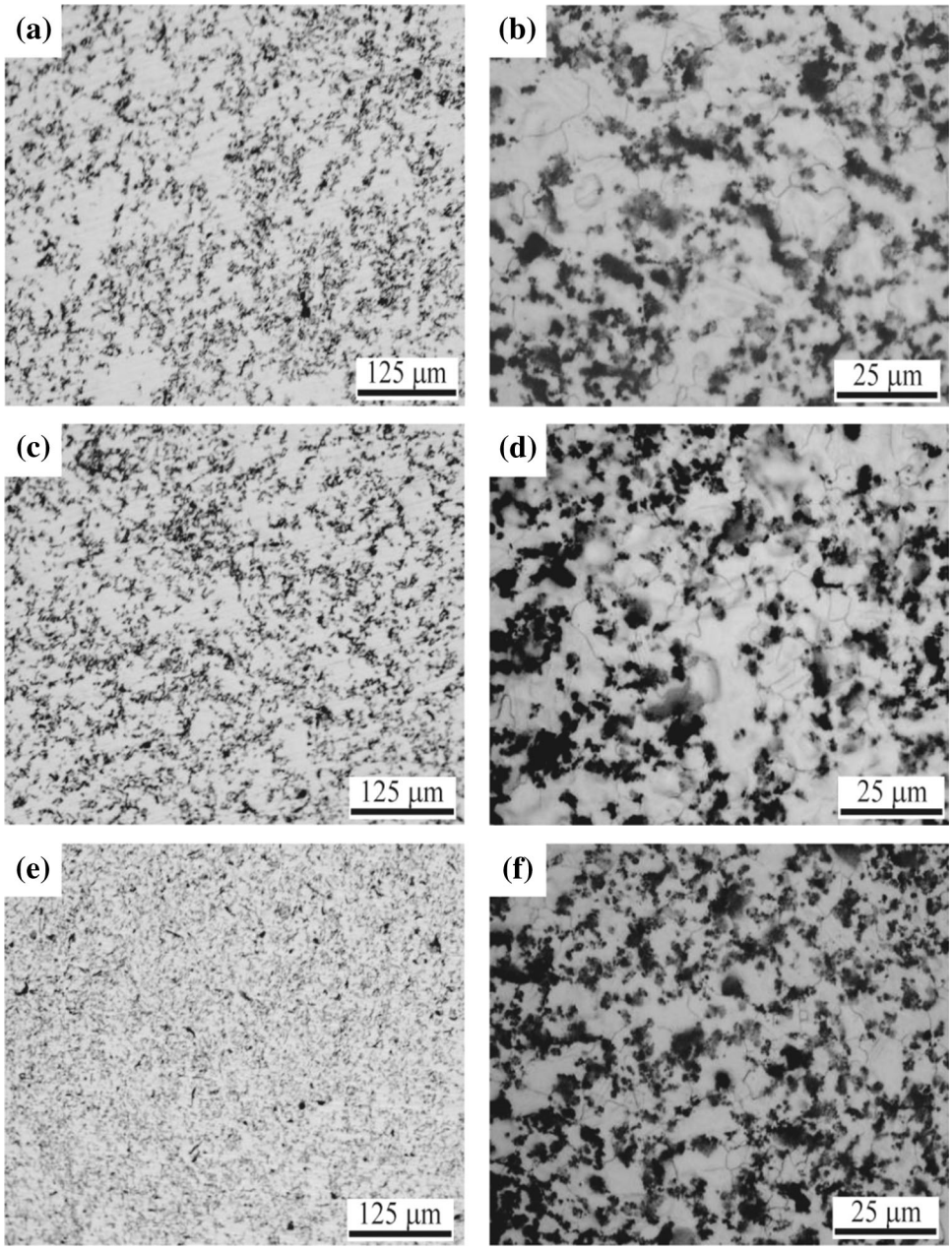

Fig. 3 OM micrographs of as-cast SiCp/AZ31B nanocomposites: (a) 1 vol.% SiCp/AZ31B nanocomposite, (b) high magnification of (a), (c) 2 vol.% SiCp/AZ31B nanocomposite, (d) high magnification of (c), (e) 3 vol.% SiCp/AZ31B nanocomposite, (f) high magnification of (e)

grain size distribution and average grain size of the SiCp/AZ31B composites after hot extrusion. Compared with the cast SiCp/AZ31B nanocomposites, there are much smaller grains in the as-extruded SiCp/AZ31B nanocomposites, as shown in Fig. 5. The finer equiaxed grains with well-defined grain boundaries indicate that the dynamic recrystallization (DRX) took place during the hot extrusion. The DRX may have initiated at the original grain boundaries (before hot extrusion) because of the accumulation of dislocations at grain boundaries during hot extrusion (Ref 14). Moreover, the grain size decreased gradually with the continuous increase of volume fraction of nano SiCp. Compared with the 2 vol.%-SiCp/AZ31B and the 3 vol.%-SiCp/AZ31B nanocomposites, the recrystallization of the 1 vol.%-SiCp/AZ31B nanocomposite is not full. In addition, the grains in the 1 vol.%-SiCp/AZ31B nanocomposites with the 24 μm-sized large grains and about 3-9 μm-sized small grains are asymmetrical, as shown in Fig. 5(a). Figure 6(a) also shows the presence of two separate peaks, as indicated by arrows in Fig. 6(a). The above results can be attributed to the following three reasons: On the one hand, the addition of nano SiCp can introduce the larger strain, which may lead to the severer DRX. On the other hand, the nano SiCp can inhibit the grain growth effectively when the grain boundaries were in touch with the particles, this will result that the grains were refined during hot extrusion, as shown in Fig. 7. Figure 7 also shows that the nano SiC particles are distributed at the grain boundary. The smaller sized SiCp could delay or hinder the recrystallization of the matrix,

which was due to the pin grain boundary effect of nano SiCp during hot deformation. Moreover, such restriction effect was enhanced as the content of nano SiCp increased to 3 vol.%.

Figure 8 shows the SEM microstructure and EDS graphs of the 3 vol.%-SiCp/AZ31B nanocomposite after hot extrusion. The nano SiCp-rich zones which were initially present in some zones in the as-cast nanocomposite disappeared in the as-extruded nanocomposite, as shown in Fig. 1 and 8(a). This means that the distribution of nano SiCp in the SiCp/AZ31B nanocomposite was significantly improved by hot extrusion. In addition, the agglomerating regions or the clusters of nano SiCp were not observed in the present SiCp/AZ31B nanocomposite with the higher volume fraction of nano SiCp (3 vol.%). The current studies have shown that it is extremely challenging for the cheapest and the simplest technique to uniformly disperse the nano SiCp of high volume content in the magnesium melts (Ref 7-9). The uniform dispersion of nano SiCp in the matrix may be not only attributed to the preparation technology, but also relates to the hot extrusion. Firstly, for all the as-cast composites, the macro-clusters of nano SiCp were not observed, and the particle distribution was relatively uniform. Secondly, the hot extrusion deformation can impel the matrix flow into the reinforcement cluster, which is due to the flow velocity of the matrix is faster than that of SiCp (Ref 15). Therefore, the distribution of micron SiCp was significantly improved after hot extrusion in the 3 vol.%-SiCp/AZ31B nanocomposites. This illustrates that the distribution of nano SiCp in the SiCp/AZ31B composites depends on the preparation technique and the hot deformation. In addition, the EDS is used to investigate the composition of the particles observed in OM and SEM, as shown in Fig. 8. Analyzing an area of SEM micrograph in Fig. 8(a), EDS of Si K and Al K (Fig. 8b and c) demonstrate that composition of particle is nano SiCp. The distribution of EDS of Si K is homogeneous in macroscopic view, which indicates that the distribution of nano SiCp is uniform in the 3 vol.% SiCp/AZ31B nanocomposite, as shown in Fig. 8(a).

Figure 9 shows the TEM images of the 3 vol.%-SiCp/AZ31B nanocomposite after hot extrusion. In Fig. 9(b) the study of electron diffraction demonstrate that composition of the particle is nano SiCp. At higher magnification, most of the nano SiCp are still segregated by magnesium matrix as shown

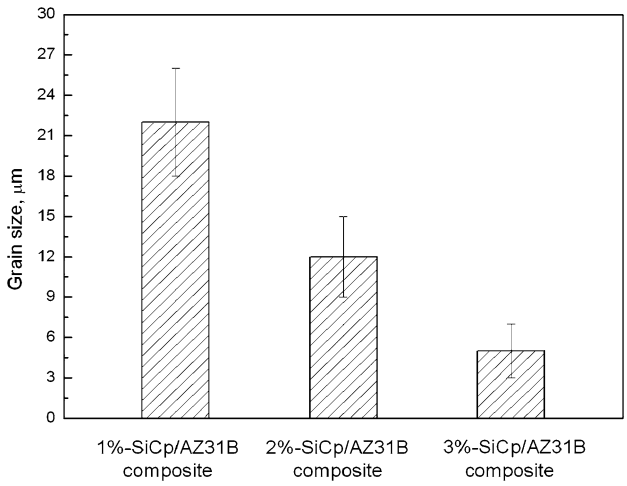

Fig. 4 Grain sizes of as-cast SiCp/AZ31B nanocomposites

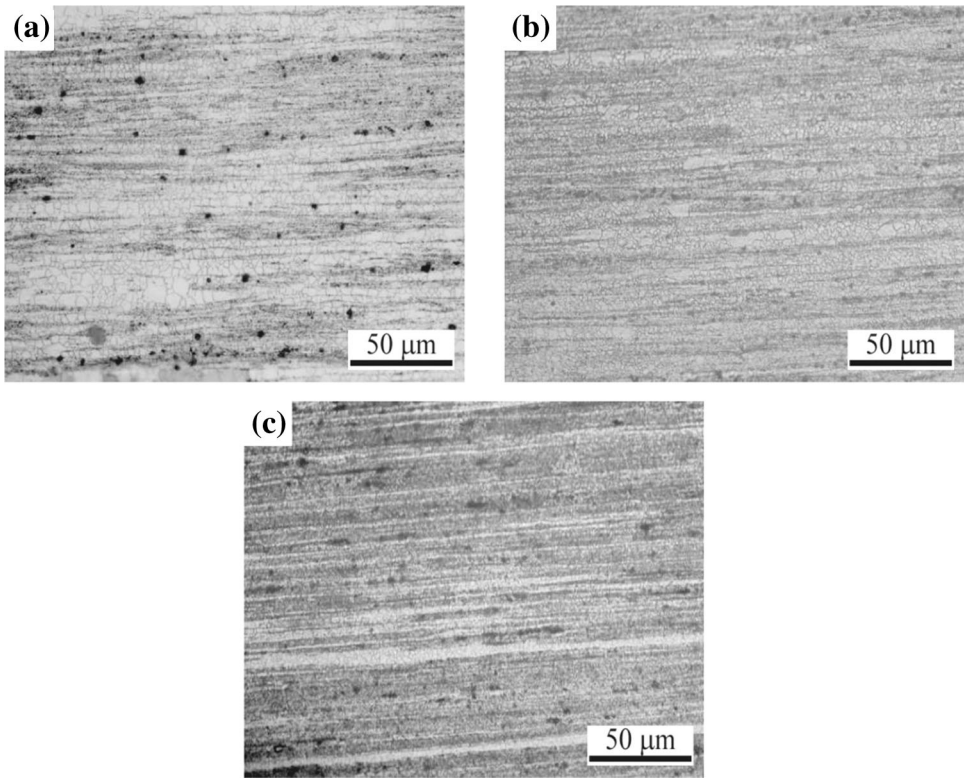

Fig. 5 OM micrographs of as-extruded SiCp/AZ31B nanocomposites: (a) 1 vol.% SiCp/AZ31B nanocomposite, (b) 2 vol.% SiCp/AZ31B nanocomposite, (c) 3 vol.% SiCp/AZ31B nanocomposite

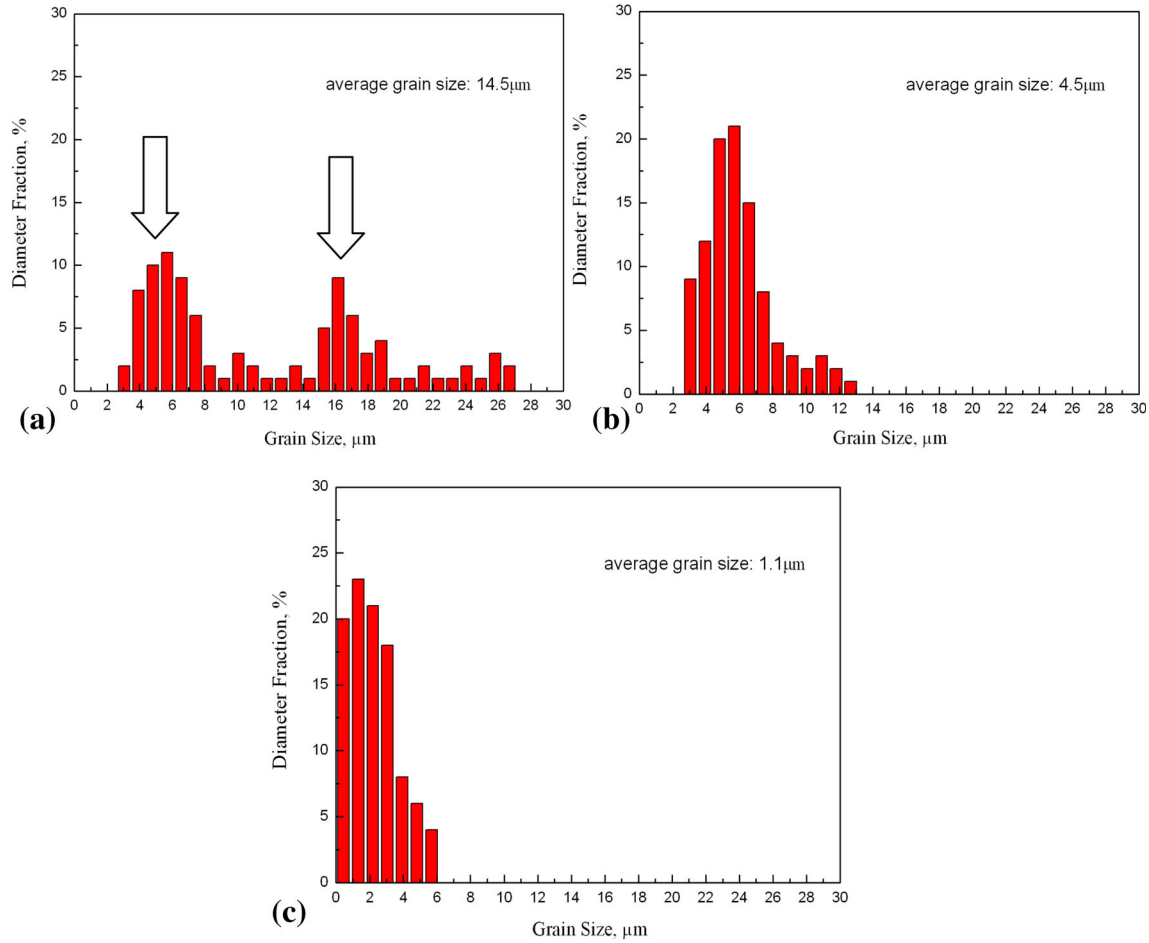

Fig. 6 Distribution of grain size for the as-extruded SiCp/AZ31B nanocomposite: (a) 1 vol.% SiCp/AZ31B nanocomposite, (b) 2 vol.% SiCp/AZ31B nanocomposite, (c) 3 vol.% SiCp/AZ31B nanocomposite

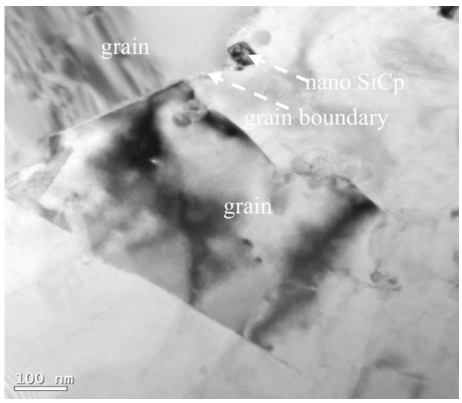

Fig. 7 TEM micrographs of the as-extruded SiCp/AZ31B nanocomposite: microstructure near nano SiCp

in Fig. 9(a). It can be also seen from Fig. 9(a) that some ultra-fine grains of about 30-60 nm exist near nano SiCp and confirmed by electron diffraction in Fig. 9(b), the grain size is much smaller than that measured by OM graph. This can further illuminate that the introduction of the 3 vol.% nano SiCp could effectively decrease the grain size. Besides, it can be demonstrated from Fig. 9 that any reaction product was not observed in the interface between the nano SiCp and matrix.

3.3 Mechanical Properties

The tensile properties of the SiCp/AZ31B nanocomposites after hot extrusion are shown in Fig. 10. Compared with the AZ31B alloy (Ref 10), the yield strength and ultimate tensile strength of the SiCp/AZ31B nanocomposites were obviously increased, while the elongation to fracture was decreased. Although, the elongation to fracture of the SiCp/AZ31B nanocomposite was decreased comparing with the as-extruded AZ31B alloy, but the elongation to fracture of the SiCp/AZ31B nanocomposite is far higher than that of the conventional magnesium matrix composites in the current literatures (Ref 15-18). The tensile strengths of monolithic material and single-sized SiCp-reinforced magnesium matrix composites are listed in Table 1. By combining Table 1 and Fig. 10, it can be found that the SiCp/AZ31B nanocomposite has much higher strength and better ductility than the conventional single-size particle (micron or nano as well as submicron)-reinforced magnesium matrix composites. For the as-extruded SiCp/AZ31B nanocomposite, the obvious improvement of the strength is mainly attributed to the dispersion strengthening of the reinforcement phase and the grain refinement of matrix (Ref 25). Firstly, the decrease of the grain size leads to the increase of the yield strength of matrix, which can be described by Hall-Petch relation (Ref 11): $\sigma_y = \sigma_0 + K_y/d^{1/2}$, where σ_0 and K_y are material constants, d is the average grain size, and σ_y is the

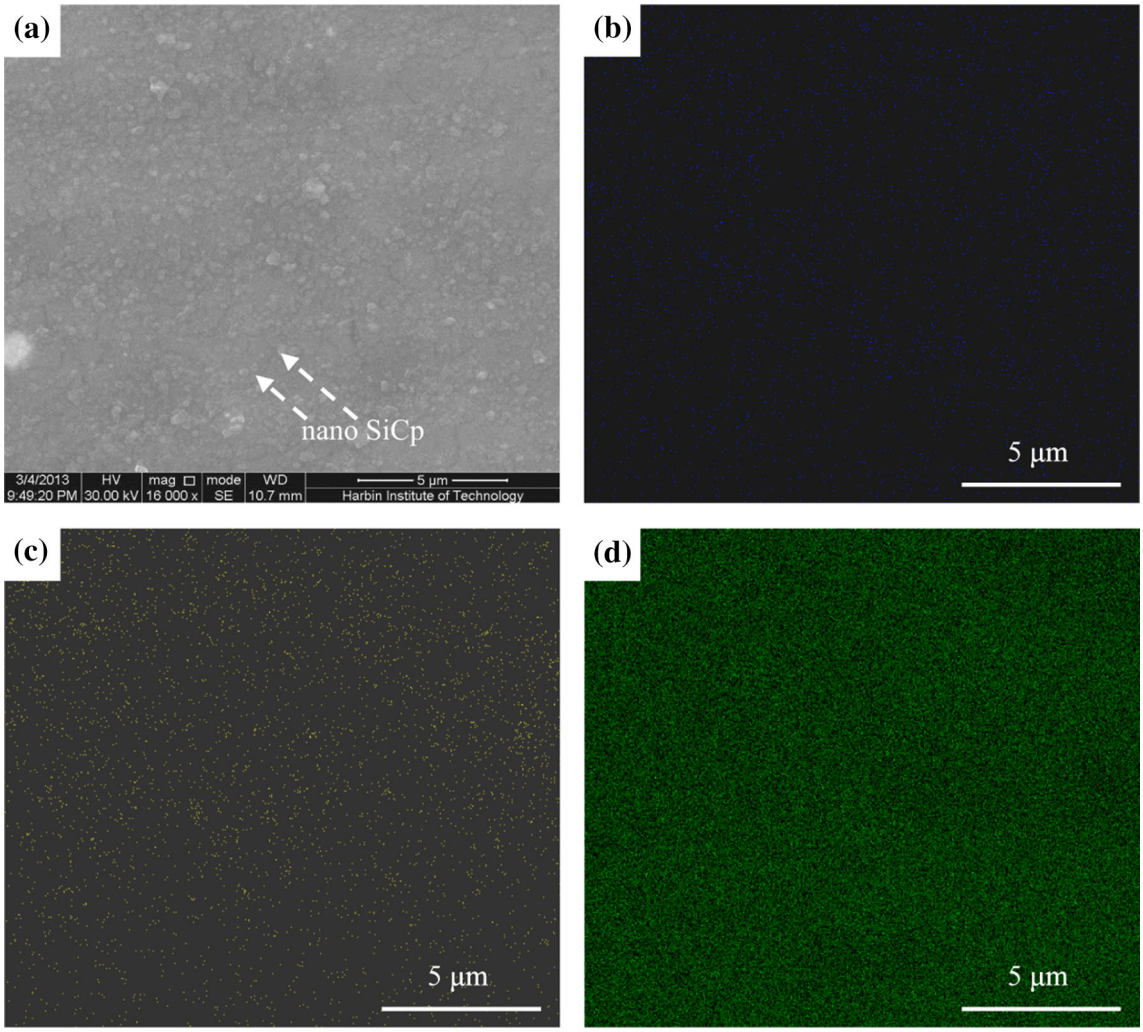

Fig. 8 SEM micrographs of (a) as-extruded 3 vol.% SiCp/AZ31B nanocomposite; EDS of (b) Al K, (c) Si K and (d) Mg K

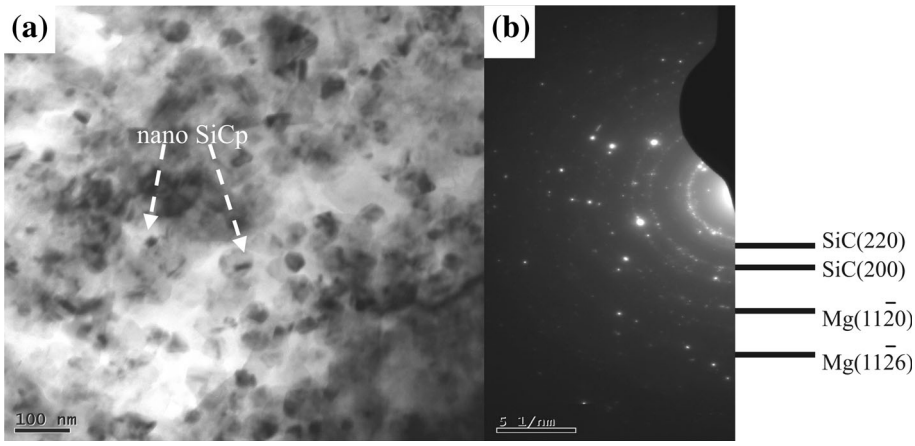

Fig. 9 TEM micrographs of the as-extruded 3 vol.%-SiCp/AZ31B nanocomposite: (a) microstructure around nano SiCp, (b) electron diffraction of nano SiCp

yield strength. The grains of matrix in the SiCp/AZ31B nanocomposite were significantly refined after hot extrusion, and the grain size decreased gradually with the continuous increase of volume fraction of nano SiCp, as shown in Fig. 5. Secondly, the geometrically necessary dislocations (GND) were generated to accommodate the mismatch of the coefficient of

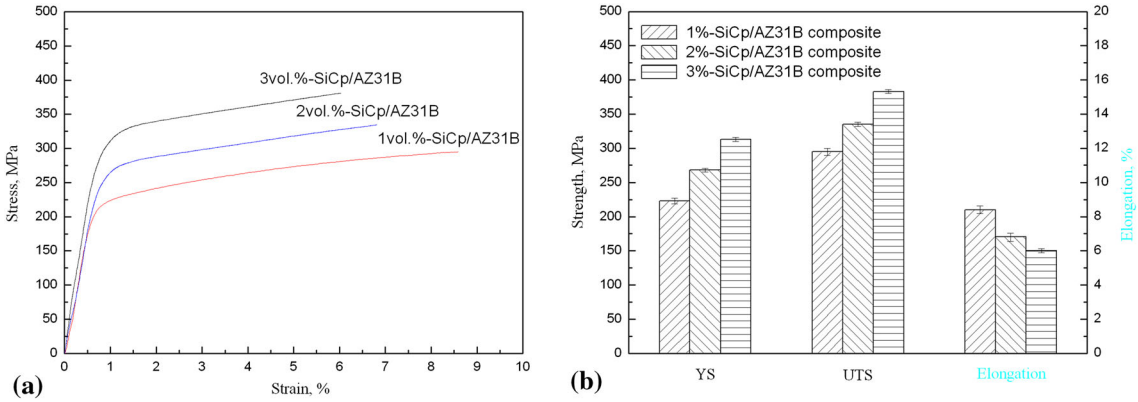

Fig. 10 The mechanical properties of SiCp/AZ31B nanocomposite after hot extrusion. (a) tensile stain–stress curves, (b) ultimate tensile strength, yield strength and elongation

Table 1 Comparison of tensile properties of magnesium-based materials

Material	0.2% YS (MPa)	UTS (MPa)	Elongation (%)
AZ31B/Al_2O_3[a,b] (Ref 19)	225 ± 3	313 ± 5	14.0 ± 1.0
AZ31/AZ91/Al_2O_3[a,b] (Ref 20)	232 ± 13	339 ± 10	15.9 ± 0.5
AZ31B/Al_2O_3-2Ca[a,b] (Ref 21)	215 ± 5	261 ± 8	10 ± 0.2
AZ31B/C-F[a,b] (Ref 20)	200	255	12
AZ51/Al_2O_3[a,b] (Ref 22)	211 ± 4	311 ± 3	13 ± 1
AZ51[a] (Ref 22)	222 ± 4	302 ± 4	9.0 + 0.4
AZ91D[a,c] (Ref 23)	215	296	10.2
AZ91D[a,d] (Ref 23)	226	313	15.6
AZ91D/15 vol.%SiCp[a,c,e] (Ref 23)	257	289	0.7
AZ91D/10 vol.%SiCp[a,d,e] (Ref 3)	260	335	4.3
AZ91D/1 vol.%SiCp[a,b,d] (Ref 9)	255	340	11.6
AZ91D/1 vol.%SiCp[a,d,f] (Ref 24)	275	345	4.0
AZ91D/15 vol.%SiCp[a,d,e] (Ref 23)	205	233	1.1

[a]Hot extrution
[b]Nano-size reinforcement
[c]Rheocast material prior to extrusion
[d]Die-cast material prior to extrusion
[e]Micron-size reinforcement
[f]Submicron-size reinforcement

thermal expansion (CTE) between the nano SiCp and matrix, which may cause the enhancement of yield strength. Thirdly, the closely spaced nano SiCp hinder the passing of dislocation by Orowan mechanism. Therefore, for the particles that the size is smaller than 1 μm, the Orowan strengthening mechanism exists in the composite. In addition, it can be seen from Fig. 8 and 9 that the nano SiCp show a relatively uniform distribution in the present work. As a result, the strength of the 3 vol.%-SiCp/AZ31B nanocomposite is significantly higher than that of other magnesium matrix composites. In contrast to the remarkable increase in the strength properties obtained by adding the nano SiCp, the obvious increase in ductility was observed in the SiCp/AZ31B nanocomposite. The reasons can be attributed to the combined effects of the following points. (1) The grain refinement: the intergranular fracture result from the inter-crystalline stress, this is well known from the previous literatures (Ref 26, 27). (2) The uniform distribution of nano SiCp along the extrusion direction: uniform distributed nano SiCp act as ductility enhancer by the pin grain boundary effect during room temperature tensile (Ref 28, 29). These uniformly distributed nano SiCp provide the sites of beneficial effect for initiating the cleavage cracks ahead of advancing crack front and help to relax the stress concentration at the crack front (Ref 20, 24). As a result, the ductility of the SiCp/AZ31B nanocomposite is significantly higher than that of the conventional micron or submicron SiCp-reinforced magnesium matrix composites. In addition, compared with the 1 vol.%-SiCp/AZ31B nanocomposites, the elongation to fractures of the 2 vol.%-SiCp/AZ31B and 3 vol.%-SiCp/AZ31B nanocomposite were slightly decreased. The reason may be attributed to the following two reasons: On the one hand, the inferior ductility of the ultra-fine grained materials with the low activity of dislocations was reported mainly due to the lack of strain hardening (Ref 30, 31). Compared with the 1 vol.%-SiCp/AZ31B nanocomposites, there are much smaller grains in the 2 vol.%-SiCp/AZ31B and 3 vol.%-SiCp/AZ31B nanocomposites after hot extrusion, as shown in Fig. 5. On the other hand, the ductility was slightly increased by developing the asymmetrical grain (coase grain: 24 μm, fine grain: 3-9 μm) in the 1 vol.%-SiCp/AZ31B nanocomposite, which increases the

strain hardening effect and acts as the crack arrester in turn improving the ductility of the composites (Ref 28, 30, 31), as shown in Fig. 5(a). In summary, the 3 vol.%-SiCp/AZ31B nanocomposite is a good choice for simultaneously achieving the good ductility and high strength in the present magnesium matrix composite.

4. Conclusions

The nano SiCp-reinforced magnesium matrix composites with high content of nano SiCp were obtained by the cheapest and the simplest technique, and then the distribution of nano SiCp and the microstructures as well as the property correlation were studied, the main conclusions can be summarized as follows:

(1) The introduction of nano-sized SiCp significantly reduced the grain size. The grain size decreased gradually with the increase of nano SiCp. The grain refinement in the SiCp/AZ31B nanocomposite is attributed to the pin grain boundary effect of nano SiCp during hot extrusion.
(2) The cheapest and the simplest melt technique is successful to solve the problem of the homodisperse of nano SiCp in the magnesium matrix. The 3 vol.% nano SiCp were uniformly dispersed by using the melt stirring technology and the hot extrusion method in the present magnesium matrix nanocomposite.
(3) Both of the yield strength and the ultimate tensile strength increased with the increase of nano SiCp volume fractions. However, compared with other SiCp/AZ31B nanocomposites, the elongation to fracture of the 3 vol.%-SiCp/AZ31B nanocomposite was slightly decreased.
(4) The high strength and good ductility of the 3 vol.%-SiCp/AZ31B nanocomposite can be attributed to the combined effects of (a) grain refinement, (b) dispersion strengthening, and (c) uniform distribution of nano SiCp.

References

1. C.R. Dandekar and Y.C. Shin, Effect of Porosity on the Interface Behavior of an Al_2O_3-Aluminum Composite: A Molecular Dynamics Study, *Compos. Sci. Technol.*, 2011, **71**, p 350–356
2. X.J. Wang, K. Wu, W.X. Huang, H.F. Zhang, M.Y. Zheng, and D.L. Peng, Study on Fracture Behavior of Particulate Reinforced Magnesium Matrix Composite Using In Situ SEM, *Compos. Sci. Technol.*, 2007, **67**, p 2253–2260
3. X.J. Wang, L. Xu, X.S. Hu, K.B. Nie, K.K. Deng, K. Wu, and M.Y. Zheng, Influences of Extrusion Parameters on Microstructure and Mechanical Properties of Particulate Reinforced Magnesium Matrix Composites, *Mater. Sci. Eng. A*, 2011, **528**, p 6387–6392
4. K.B. Nie, X.J. Wang, X.S. Hu, Y.W. Wu, K.K. Deng, K. Wu, and M.Y. Zheng, Effect of Multidirectional Forging on Microstructures and Tensile Properties of a Particulate reinforced Magnesium Matrix Composite, *Mater. Sci. Eng. A*, 2011, **528**, p 7133–7139
5. X.J. Wang, N.Z. Wang, L.Y. Wang, X.S. Hu, K. Wu, Y.Q. Wang, and Y.D. Huang, Processing, Microstructure and Mechanical Properties of Micro-SiC Particles Reinforced Magnesium Matrix Composites Fabricated by Stir Casting Assisted by Ultrasonic Treatment Processing, *Mater. Des.*, 2014, **57**, p 638–645
6. W.L.E. Wong and M. Gupta, Development of Mg/Cu Nanocomposites Using Microwave Assisted Rapid Sintering, *Compos. Sci. Technol.*, 2007, **67**, p 1541–1552
7. S.F. Hassan, Effect of Primary Processing Techniques on the Microstructure and Mechanical Properties of Nano-Y_2O_3 Reinforced Magnesium Nanocomposites, *Mater. Sci. Eng. A*, 2011, **528**, p 5484–5490
8. S.F. Hassan and M. Gupta, Development of High Performance Magnesium Nano-composites Using Nano-Al_2O_3 as Reinforcement, *Mater. Sci. Eng. A*, 2005, **392**, p 163–168
9. K.B. Nie, X.J. Wang, L. Xu, K. Wu, X.S. Hu, and M.Y. Zheng, Effect of Hot Extrusion on Microstructures and Mechanical Properties of SiC Nanoparticles Reinforced Magnesium Matrix Composite, *J. Alloys Compd.*, 2012, **512**, p 355–360
10. M.J. Shen, X.J. Wang, C.D. Li, M.F. Zhang, X.S. Hu, M.Y. Zheng, and K. Wu, Effect of Bimodal Size SiC Particulates on Microstructure and Mechanical Properties of AZ31B Magnesium Matrix Composites, *Mater. Des.*, 2013, **52**, p 1011–1017
11. M.J. Shen, X.J. Wang, M.F. Zhang, X.S. Hu, M.Y. Zheng, and K. Wu, Fabrication of Bimodal Size SiCp Reinforced AZ31B Magnesium Matrix Composites, *Mater. Sci. Eng. A*, 2014, **601**, p 58–64
12. K.K. Deng, K. Wu, X.J. Wang, Y.W. Wu, X.S. Hu, M.Y. Zheng, W.M. Gan, and H.G. Brokmeier, Microstructure Evolution and Mechanical Properties of a Particulate Reinforced Magnesium Matrix Composites Forged at Elevated Temperatures, *Mater. Sci. Eng. A*, 2010, **527**, p 1630–1635
13. K.K. Deng, X.J. Wang, W.M. Gan, Y.W. Wu, K.B. Nie, K. Wu, M.Y. Zheng, and H.G. Brokmeier, Isothermal Forging of AZ91 Reinforced with 10 vol.% Silicon Carbon Particles, *Mater. Sci. Eng. A*, 2011, **528**, p 1707–1712
14. B. Cicek, H. Ahlatc, and Y. Sun, Wear Behaviours of Pb Added Mg-Al-Si Composites Reinforced with In Situ Mg2Si Particles, *Mater. Des.*, 2013, **50**, p 929–935
15. K.B. Nie, K. Wu, X.J. Wang, K.K. Deng, Y.W. Wu, and M.Y. Zheng, Multidirectional Forging of Magnesium Matrix Composites: Effect on Microstructures and Tensile Properties, *Mater. Sci. Eng. A*, 2010, **527**, p 7364–7368
16. K.B. Nie, X.J. Wang, K. Wu, X.S. Hu, M.Y. Zheng, and L. Xu, Microstructure and Tensile Properties of micro-SiC Particles Reinforced Magnesium Matrix Composites Produced by Semisolid Stirring Assisted Ultrasonic Vibration, *Mater. Sci. Eng. A*, 2011, **528**, p 8709–8714
17. K.K. Deng, X.J. Wang, M.Y. Zheng, and K. Wu, Dynamic Recrystallization Behavior During Hot Deformation and Mechanical Properties of 0.2 μm SiCp Reinforced Mg Matrix Composite, *Mater. Sci. Eng. A*, 2013, **560**, p 824–830
18. W.S. Miller and F.J. Humphreys, Strengthening Mechanisms in Particulate Metal Matrix Composites, *Scr. Mater.*, 1991, **25**, p 33–38
19. M. Paramsothy, Q.B. Nguyen, K.S. Tun, J. Chan, R. Kwok, J.V.M. Kuma, and M. Gupta, Mechanical Property Retention in Remelted Microparticle to Nanoparticle AZ31/Al_2O_3 Composites, *J. Alloys Compd.*, 2010, **506**, p 600–606
20. M. Paramsothy, J. Chan, R. Kwok, and M. Gupta, The Synergistic Ability of Al_2O_3 Nanoparticles to Enhance Mechanical Response of Hybrid Alloy AZ31/AZ91, *J. Alloys Compd.*, 2011, **509**, p 7572–7578
21. Q.B. Nguyen and M. Gupta, Microstructure and Mechanical Characteristics of AZ31B/Al_2O_3 Nano-composite with Addition of Ca, *J. Compos. Mater.*, 2009, **43**, p 5–17
22. M.E. Alam, A.M.S. Hamouda, and M. Gupta, Microstructure, Thermal and Mechanical Response of AZ51/Al_2O_3 Nanocomposite with 2 wt.% Ca Addition, *Mater. Des.*, 2013, **50**, p 1–6
23. M. Paramsothy, S.F. Hassan, N. Srikanth, and M. Gupta, Enhancing Tensile/Compressive Response of Magnesium Alloy AZ31 by Integrating with Al_2O_3 Nanoparticles, *Mater. Sci. Eng. A*, 2009, **527**, p 162–168
24. K.K. Deng, K. Wu, Y.W. Wu, K.B. Nie, and M.Y. Zheng, Effect of Submicron Size SiC Particulates on Microstructure and Mechanical Properties of AZ91 Magnesium Matrix Composites, *J. Alloys Compd.*, 2010, **504**, p 542–547
25. M.C. Zhao, F.X. Yin, T. Hanamura, H. Qiu, K. Nagai, and A. Atrens, Relationship Between Yield Strength and Grain Size for a Bimodal Structural Ultrafine-Grained Ferrite/Cementite Steels, *Scr. Mater.*, 2007, **57**, p 857–860

26. J. Koike, Enhanced Deformation Mechanisms by Anisotropic Plasticity in Polycrystalline Mg Alloys at Room Temperature, *Metall. Mater. Trans. A*, 2005, **36**, p 1689–1696
27. M.C. Zhao, Y.L. Deng, and X.M. Zhang, Strengthening and Improvement of Ductility Without Loss of Corrosion Perforation in a Magnesium Alloy by Homogenizing Annealing, *Scr. Mater.*, 2008, **58**, p 560–563
28. S. Sankaranarayanan, R.K. Sabat, S. Jayalakshmi, S. Suwas, and M. Gupta, Effect of Nanoscale Boron Carbide Particle Addition on the Microstructural Evolution and Mechanical Response of Pure Magnesium, *Mater. Des.*, 2014, **56**, p 428–436
29. M.C. Zhao, T. Hanamura, H. Qiu, and K. Yang, Low Absorbed Energy Ductile Dimple Fracture in Lower Shelf Region in an Ultrafine Grained Ferrite/Cementite Steel, *Metall. Mater. Trans. A*, 2006, **37**, p 2897–2990
30. M.C. Zhao, T. Hanamura, H. Qiu, K. Nagai, and K. Yang, Dependence of Strength and Strength-Elongation Balance on the Volume Fraction of Cementite Particles in Ultrafine Grained Ferrite/Cementite Steels, *Scr. Mater.*, 2006, **54**, p 1385–1389
31. T. Hirano, T. Ohji, and K. Niihara, Effect of Matrix Grain Size on the Mechanical Properties of Si_3N_4/SiC Nanocomposites Densified with Y_2O_3, *Mater. Lett.*, 1996, **27**, p 53–58